

# Temporal filtering by double diffraction

Jürgen Jahns and Adolf W. Lohmann

We present a theoretical analysis of the temporal behavior of double-diffraction setups. It applies, in particular, to Talbot and Montgomery interferometers, whose operation is based on the self-imaging effect. The use of both types of interferometer as temporal filters for optical and terahertz applications was recently suggested. We show that double-diffraction setups can be modeled as communications channels with dispersive behavior caused by diffraction. We develop mathematical expressions for the phase delay, the group velocity, and the group-velocity dispersion for both quasi-monochromatic and polychromatic case. Based on these results, the temporal impulse response of a double-diffraction setup is derived. Finally, a general description of its practical implementation are presented. © 2004 Optical Society of America

OCIS codes: 050.1970, 070.6020, 070.6760.

## 1. Introduction: The Optical Setup

Double-diffraction experiments based on the Talbot and the Lau effects<sup>1,2</sup> were shown to be useful, for example, in building interferometers for the analysis of spatial objects.<sup>3,4</sup> Recently Jahns *et al.*<sup>5,6</sup> suggested considering double-diffraction experiments also for the temporal filtering of optical signals. In those papers, however, the theoretical analysis of the experiments was based on behavior in the spatial domain. Temporal behavior was implicitly introduced in terms of path-length differences. This point of view is limited, however, to the monochromatic and stationary case and does not allow one an in-depth analysis of the temporal behavior of the interferometers. Hence it is necessary to develop a mathematical framework for the description of double-diffraction setups to explain their temporal characteristics. That is the purpose of this paper.

Temporal filtering requires the implementation of well-defined time delays. The implementation of time delays by interferometric devices (e.g., by a Michelson interferometer) has a long tradition. Our approach differs significantly in that we use not two-

way interferometers but multiple-beam interferometers acting as beam splitters, diffraction gratings, or modifications thereof.

The basic experimental setup to be analyzed is shown in Fig. 1. It consists of two optical components (called masks),  $M_1$  and  $M_2$ , separated by a finite distance,  $z_0$ . The wave field that emerges behind  $M_2$  is spatially filtered such that only the component traveling parallel to the optical axis passes through the exit pupil. Depending on the spatial structure of masks  $M_1$  and  $M_2$ , we distinguish among three cases described below. Note that, in what follows, we use a one-dimensional representation for simplicity. A tilde denotes a Fourier transform,  $x$  is the spatial coordinate,  $\nu$  is the spatial frequency, and  $\nu_t$  is the temporal frequency.

Case 1 is a general case, where  $M_1$  and  $M_2$  are continuous objects mathematically described as

$$M_1(x) = \int A(\nu) \exp(2\pi i \nu x) d\nu, \quad A(\nu) = \tilde{M}_1(\nu), \quad (1)$$

$$M_2(x) = \int B(\nu) \exp(2\pi i \nu x) d\nu, \quad B(\nu) = \tilde{M}_2(\nu). \quad (2)$$

Case 2 comprises periodic masks, as used in the Talbot case:

$$M_1(x) = \sum_m A_m \exp(2\pi i m \nu_0 x),$$
$$\tilde{M}_1(\nu) = \sum_{-N/2}^{N/2-1} A_m \delta(\nu - m \nu_0), \quad (3)$$

J. Jahns (jahns@fernuni-hagen.de) is with Optische Nachrichtentechnik, Fern Universität Hagen, Universitätsstrasse 27/PRG, 58084 Hagen, Germany. A. W. Lohmann is with the Lehrstuhl für Nachrichtentechnik, Universität Erlangen-Nürnberg, Cauerstrasse 7, 91058 Erlangen, Germany.

Received 11 November 2003; revised manuscript received 6 May 2004; accepted 10 May 2004.

0003-6935/04/224339-06\$15.00/0

© 2004 Optical Society of America

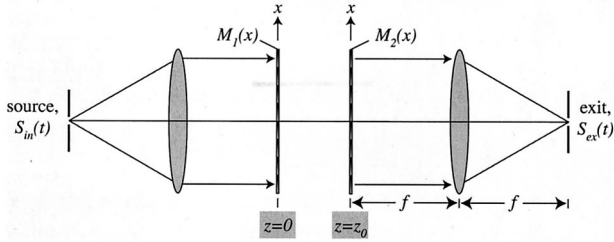


Fig. 1. Optical double-diffraction setup with masks  $M_1$  and  $M_2$ . The optical output is observed in the zeroth order behind  $M_2$ .

$$M_2(x) = \sum_n B_n \exp(2\pi i n \nu_0 x) \text{ and}$$

$$\tilde{M}_2(\nu) = \sum_{-N/2}^{N/2-1} B_n \delta(\nu - n \nu_0). \quad (4)$$

Note that the same spatial period  $p = 1/\nu_0$  is assumed for both masks.

Case 3 includes quasi-periodic masks as used for the Montgomery interferometer<sup>6,7</sup>:

$$\tilde{M}_1(\nu) = A_0 + \sum_{m>0} A_m \delta(\nu - \sqrt{m} \nu_0) + \sum_{m<0} A_m \delta(\nu - \sqrt{|m|} \nu_0), \quad (5)$$

$$\tilde{M}_2(\nu) = B_0 + \sum_{n>0} B_n \delta(\nu - \sqrt{n} \nu_0) + \sum_{n<0} B_n \delta(\nu - \sqrt{|n|} \nu_0). \quad (6)$$

## 2. Theoretical Analysis: from the Monochromatic Source to the Exit

In this section we calculate the optical field at the exit pupil as a function of time. To simplify the analysis we limit ourselves to one lateral coordinate,  $x$ . In what follows, we assume the validity of scalar diffraction theory and the paraxial approximation. Furthermore, we consider first the idealized case of quasi-monochromatic illumination at a specific frequency  $\nu_t$ , i.e., one component of the spectrum mathematically represented as

$$S_{in}(t) = \exp(-2\pi i \nu_t t). \quad (7)$$

Below, we extend our analysis to polychromatic illumination.

Let the first mask,  $M_1$ , be located in the plane  $z = 0$ . Immediately behind the first mask, i.e., for  $z = +0$ , the complex amplitude  $u(x, z = +0, t)$  is given as

$$u(x, z = +0, t) = S_{in}(t) M_1(x) = \int \tilde{M}_1(\nu) \exp[2\pi i(\nu x - \nu_t t)] d\nu. \quad (8)$$

For  $z > 0$  we obtain the field by multiplying the angular spectrum by a propagation factor  $\exp(2\pi i \beta z)$ :

$$u(x, z > 0, t) = \int \tilde{M}_1(\nu) \exp[2\pi i(\nu x + \beta z - \nu_t t)] d\nu. \quad (9)$$

Note that the letter  $\beta$  was chosen here because it is reminiscent of the propagation constant, despite the fact that it is different by a factor of  $2\pi$ . One can derive  $\beta$  by inserting Eq. (9) into the wave equation:

$$\left( \Delta_{xz} - \frac{1}{c^2} \frac{\partial}{\partial t^2} \right) u(x, z, t) = 0. \quad (10)$$

Here  $\Delta_{xz}$  is the two-dimensional Laplace operator in  $x$  and  $z$ . Combination of Eqs. (9) and (10) yields

$$(2\pi i)^2 \int \tilde{M}_1(\nu) \left[ \nu^2 + \beta^2 - \left( \frac{\nu_t}{c} \right)^2 \right] \exp[2\pi i(\nu x + \beta z - \nu_t t)] d\nu = 0. \quad (11)$$

Because Eq. (11) has to hold for arbitrary values of  $z$  and  $t$ , the expression in braces has to be equal to zero, or

$$\beta^2 = (\nu_t/c)^2 - \nu^2. \quad (12)$$

Immediately before mask  $M_2$ , the field is therefore given as

$$u(x, z = z_0 - 0, t) = \int \tilde{M}_1(\nu) \exp[2\pi i(\nu x + \beta z_0 - \nu_t t)] d\nu, \quad (13)$$

with  $\beta = [(\nu_t/c)^2 - \nu^2]^{1/2}$ . The root is real if evanescent waves are ignored, and behind  $M_2$  it is

$$u(x, z = z_0 + 0, t) = \iint \tilde{M}_1(\nu_1) \tilde{M}_2(\nu_2) \exp[2\pi i\{(\nu_1 + \nu_2)x + \beta z_0 - \nu_t t\}] d\nu_1 d\nu_2. \quad (14)$$

The field in the exit plane  $z = z_0 + 2f$  is given as the Fourier transform of  $u(x, z_0 + 0, t)$  with respect to spatial coordinate  $x$ . We call the lateral coordinate in the output plane  $x'$ . Then

$$u(x', z_0 + 2f, t) = \int u(x, z_0 + 0, t) \exp(-2\pi i x x' / \lambda f) dx = \iiint \tilde{M}_1(\nu_1) \tilde{M}_2(\nu_2) \exp(2\pi i\{x[\nu_1 + \nu_2 - x'(\nu_t/cf)] + \beta z_0 - \nu_t t\}) d\nu_1 d\nu_2 dx. \quad (15)$$

The integration over  $x$  yields  $\int \dots dx = \delta[\nu_1 + \nu_2 - x'(\nu_t/cf)]$ ; the subsequent integration over  $\nu_2$  results

in transformation of the frequency coordinate:  $\nu_2 \rightarrow x'(\nu_t/cf) - \nu_1$ . To simplify the following expression, we omit the term ( $\nu = \nu_1$ ) and write  $\nu' = x'(\nu_t/cf)$ . With this we obtain

$$u(x', z_0 + 2f, t) = \int \tilde{M}_1(\nu)\tilde{M}_2(\nu' - \nu) \times \exp[2\pi i(\beta z_0 - \nu_t t)] d\nu. \quad (16)$$

The exit pupil is located at  $x' = 0$ ; hence

$$u_{\text{ex}}(t) = u(0, z_0 + 2f, t) = \int \tilde{M}_1(\nu)\tilde{M}_2(-\nu)\exp[2\pi i(\beta z_0 - \nu_t t)] d\nu. \quad (17)$$

Using

$$\beta = \left[ \left( \frac{\nu_t}{c} \right)^2 - \nu^2 \right]^{1/2} = \frac{\nu_t}{c} - \left\{ \frac{\nu_t}{c} - \left[ \left( \frac{\nu_t}{c} \right)^2 - \nu^2 \right]^{1/2} \right\}, \quad (18)$$

we can rewrite Eq. (17) as

$$\begin{aligned} u_{\text{ex}}(t) &= \int \tilde{M}_1(\nu)\tilde{M}_2(-\nu)\exp\left[2\pi i\left(\nu_t\left(\frac{z_0}{c} - t\right) - z_0\left\{\frac{\nu_t}{c} - \left[ \left( \frac{\nu_t}{c} \right)^2 - \nu^2 \right]^{1/2} \right\}\right)\right] d\nu \\ &= \int \tilde{M}_1(\nu)\tilde{M}_2(-\nu)\exp\left[2\pi i\nu_t\left(\frac{z_0}{c} - t\right) - i\varphi_D(\nu)\right] d\nu. \end{aligned} \quad (19)$$

In the exponent, the first term  $2\pi\nu_t[(z_0/c) - t]$ , is the phase delay that is due to propagation in the  $z$  direction and

$$\varphi_D(\nu) = 2\pi z_0 \left\{ \frac{\nu_t}{c} - \left[ \left( \frac{\nu_t}{c} \right)^2 - \nu^2 \right]^{1/2} \right\} \quad (20)$$

is the phase delay that is due to diffractive dispersion. The analogy between the diffraction blur in the spatial domain and the group-velocity dispersion in the time domain was pointed out earlier in Ref. 8. Here we present a result that links the two effects. In any optical system that is spatially multimodal (i.e., with an extended angular spectrum), a temporal blur is introduced if we consider propagation along one specific direction (e.g., along the optical axis, as in our case). By rearranging Eq. (20) we may also write

$$\beta = \frac{\nu_t}{c} - \frac{\varphi_D}{2\pi z_0}. \quad (21)$$

The inverse of the derivative of the propagation constant with respect to the temporal frequency is

known as the group velocity  $v_g$  of the light signal.<sup>9</sup> In our notation it is

$$\frac{1}{v_g} = \frac{\partial\beta}{\partial\nu_t} = \frac{1}{c} - \frac{1}{2\pi z_0} \frac{\partial\varphi_D}{\partial\nu_t}. \quad (22)$$

Dispersive constant  $D$  (or the group-velocity dispersion) is given as

$$D = \frac{\partial^2\beta}{\partial\nu_t^2}. \quad (23)$$

### 3. Case Study

In this section we consider three specific cases as listed in Section 1: (1) i.e., the general case; (2)  $M_1$  and  $M_2$  are arbitrary,  $M_1$  and  $M_2$  are linear gratings of the same period  $1/\nu_0$ ; (3)  $M_1$  and  $M_2$  are quasi-periodic functions.

*Case 1 (general case).* Starting from Eq. (19) and using the following approximation:

$$\begin{aligned} \left[ \left( \frac{\nu_t}{c} \right)^2 - \nu^2 \right]^{1/2} &= \frac{\nu_t}{c} \left[ 1 - \left( \frac{\nu c}{\nu_t} \right)^2 \right]^{1/2} \\ &\approx \frac{\nu_t}{c} \left[ 1 - \frac{1}{2} \left( \frac{\nu c}{\nu_t} \right)^2 \right], \end{aligned} \quad (24)$$

we obtain the following expression for the diffractive delay:

$$\varphi_D(\nu) \approx -\pi \frac{cz_0}{\nu_t} \nu^2. \quad (25)$$

We now develop  $1/\nu_t$  into a Taylor series about a center frequency  $\bar{\nu}_t$ . With  $\nu_t = \nu'_t - \bar{\nu}_t$ , we obtain

$$\frac{1}{\nu_t} \approx \frac{1}{\bar{\nu}_t} \left( 2 - \frac{\nu'_t}{\bar{\nu}_t} \right); \quad (26)$$

hence we can write

$$\varphi_D(\nu) \approx -2\pi \frac{cz_0}{\bar{\nu}_t} \left( 1 - \frac{\nu'_t}{2\bar{\nu}_t} \right) \nu^2. \quad (27)$$

Notable in expression (27) is the quadratic dependency of the dispersive delay on spatial frequency coordinate  $\nu$ . With Eq. (22) and expression (25) we can derive the following expression for the group velocity:

$$v_g^{(1)} \approx \frac{2c\nu_t^2}{2\nu_t^2 + (c\nu)^2}, \quad (28)$$

and for the dispersion constant:

$$D^{(1)} = -\frac{4\nu_t^3}{c\nu^2}. \quad (29)$$

*Case 2 (linear gratings).* We use Eqs. (3) and (4) and assume that  $B_{-m} = A_m^*$ . This is not a necessary condition, in general. However, it describes the situation of the Talbot and Montgomery interferometers as time filters, for which two complementary phase masks are used; see Fig. 2 and Refs. 5 and 6. We can

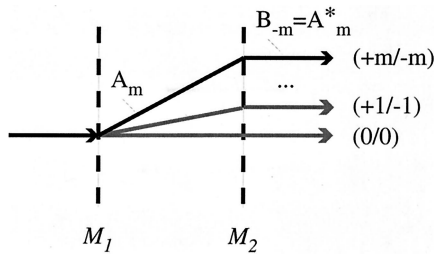


Fig. 2. Paths of the different orders in the double-diffraction experiment. The zeroth order behind  $M_2$  is composed of the combined orders (0/0), (1, -1), etc., where the first digit is the index of the diffraction order generated by  $M_1$ .  $A_m$  and  $B_m$  are the amplitudes of the respective diffraction orders.

then show, by inserting the expressions for  $\tilde{M}_1(\nu)$  and  $\tilde{M}_2(\nu)$  and by evaluating the integral over  $\nu$ , that

$$u_{\text{ex}}(t) = \sum |A_m|^2 \exp \left\{ i \left[ 2\pi \nu_t \left( \frac{z_0}{c} - t \right) - \varphi_{D,m}(\nu) \right] \right\}, \quad (30)$$

with

$$\varphi_{D,m}(\nu) = -\pi \frac{cz_0}{\nu_t} (m\nu_0)^2. \quad (31)$$

With expression (26) we may write

$$\varphi_{D,m}(\nu) \approx -2\pi \frac{cz_0}{\bar{\nu}_t} \left( 1 - \frac{\nu'_t}{2\bar{\nu}_t} \right) (m\nu_0)^2. \quad (32)$$

The group velocity in this case is

$$v_g^{(2)} \approx \frac{2c\nu_t^2}{2\nu_t^2 + (m\nu_0)^2}, \quad (33)$$

and the dispersion constant is

$$D^{(2)} = -\frac{4\nu_t^3}{c(m\nu_0)^2}. \quad (34)$$

Because spatial period  $1/\nu_0$  will, in general, be (much) larger than the center wavelength of the light ( $c/\bar{\nu}_t$ ), we can approximate expression (33) as

$$v_g^{(2)} \approx c \left[ 1 - \left( m \frac{\nu_p}{\nu_0} \right)^2 \right], \quad \nu_p = c/p.$$

*Case 3 (quasi-periodic Montgomery object).* We find the following expression for the diffractive delay:

$$\varphi_{D,m}(\nu) = -\pi \frac{cz_0}{\nu_t} m\nu_0^2 \approx -2\pi \frac{cz_0}{\bar{\nu}_t} \left( 1 - \frac{\nu'_t}{2\bar{\nu}_t} \right) m\nu_0^2. \quad (35)$$

The important difference from Eq. (31) in describing linear gratings is that the propagation constant and hence the diffractive phase delay is now linear in  $m$ . Accordingly, it is

$$v_g^{(3)} = \frac{2c\nu_t^2}{2\nu_t^2 + m(c\nu_0)^2} \approx c \left[ 1 - m \left( \frac{\nu_p}{\nu_t} \right)^2 \right], \quad (36)$$

and

$$D^{(3)} = -\frac{4\nu_t^3}{cm\nu_0^2}. \quad (37)$$

#### 4. Polychromatic Illumination and Temporal Impulse Response

So far we have considered the response to monochromatic input. Here we want to derive the equations for polychromatic response  $U(t)$  for an arbitrary input source characterized by its spectrum  $\tilde{S}(\nu_t)$ , which is centered about  $\bar{\nu}_t$ .  $U(t)$  is given as

$$U(t) = \int \tilde{S}(\nu_t) u_{\text{ex}}(t; \nu_t) d\nu_t. \quad (38)$$

We may again distinguish among our three cases; however, we shall limit the discussion to the interesting cases, 2 and 3. Using expression (26) and Eqs. (30) and (31), we can express both by

$$u_{\text{ex}}(t) = \sum |A_m|^2 \int \tilde{S}(\nu'_t - \bar{\nu}_t) \exp \{ 2\pi i [\beta_m(\nu'_t) z_0 - (\nu'_t - \bar{\nu}_t)t] \} d\nu'_t, \quad (39)$$

with

$$\beta_m = \frac{\nu'_t - \bar{\nu}_t}{c} - \frac{c}{\bar{\nu}_t} \left( 1 - \frac{\nu'_t}{\bar{\nu}_t} \right) \rho_m^2, \quad (40)$$

$$\rho_m^2 = \begin{cases} m^2 \nu_0^2 & \text{(case 2)} \\ m \nu_0^2 & \text{(case 3)} \end{cases}.$$

The exponent in brackets in Eq. (39) can be written as

$$\{ \dots \} = \left( \bar{\nu}_t t - \bar{\nu}_t \frac{z_0}{c} - \frac{c\rho_m^2 z_0}{\bar{\nu}_t} \right) - \nu'_t \left( t - \frac{z_0}{c} - \frac{c\rho_m^2 z_0}{2\bar{\nu}_t^2} \right). \quad (41)$$

The first expression can be pulled out of the integral in Eq. (39). The terms that depend on  $\nu'_t$  are

$$\int \tilde{S}(\nu'_t - \bar{\nu}_t) \exp \left[ -2\pi i \nu'_t \left( t - \frac{z_0}{c} - \frac{c\rho_m^2 z_0}{2\bar{\nu}_t^2} \right) \right] d\nu'_t$$

$$= \exp \left[ -2\pi i \bar{\nu}_t \left( t - \frac{z_0}{c} - \tau_m \right) \right] S \left( t - \frac{z_0}{c} - \tau_m \right), \quad (42)$$

with

$$\tau_m = \begin{cases} m^2 \tau_1 & \text{(case 2)} \\ m \tau_1 & \text{(case 3)} \end{cases}, \quad (43)$$

$$\tau_1 = \frac{c\nu_0^2 z_0}{2\bar{\nu}_t^2}. \quad (44)$$

Overall, we obtain for the temporal output,  $U(t)$ ,

$$U(t) = \sum |A_m|^2 \exp(-2\pi i \bar{\nu}_t \tau_m) S(t - \tau_m). \quad (45)$$

Here the trivial time shift  $z_0/c$  that is due to propagation was omitted.

The temporal impulse response, denoted  $U_{\delta}(t)$ , of a double-diffraction setup is derived for  $\tilde{S}(v_t) = \text{constant}$ . For simplicity, one can set the constant to be equal to 1. Then the integral in Eq. (42) yields

$$\int \tilde{S}(v_t) \dots dv_t' = \int \exp[-2\pi i v_t'(t - \tau_m)] dv_t' = \delta(t - \tau_m). \quad (46)$$

The impulse response, denoted  $U_{\delta}(t)$ , is then determined to be

$$U_{\delta}(t) = \sum |A_m|^2 \exp\left(2\pi i \rho_m^2 \frac{\bar{v}_t}{c} z_0\right) \delta(t - \tau_m). \quad (47)$$

With these equations we have now a relationship between the temporal impulse response and the experimental parameters in a double-diffraction setup. To make this point clear, we may make the replacements  $v_0 \rightarrow 1/p$  (spatial period) and  $\bar{v}_t/c = \bar{\lambda}$  (central wavelength of illumination) to write

$$\tau_1 = \frac{z_0 \bar{\lambda}}{z_T c}. \quad (48)$$

Here  $z_T = 2p^2/\bar{\lambda}$  is the well-known Talbot distance for self-imaging for monochromatic illumination of wavelength  $\bar{\lambda} = c/\bar{v}_t$ . For  $z_0 = Mz_T$  ( $M = 1, 2, 3 \dots$ ) the time delay of the  $m$ th diffraction order relative to the zeroth order is given by  $m^2 M \bar{\lambda}/c$  (case 2) and by  $mM \bar{\lambda}/c$  (case 3). Then the phase factor in the impulse response becomes unity, simplifying the result to

$$U_{\delta}(t) = \sum |A_m|^2 \delta(t - \tau_m), \quad (49)$$

with

$$\tau_m = m^2 \tau_1 \quad (\text{case 2}), \quad (50a)$$

$$\tau_m = m \tau_1 \quad (\text{case 3}). \quad (50b)$$

Equation (49) gives the impulse response for the polychromatic case; however, it is important to note that we have made simplifying assumptions to obtain this result. In particular, we have assumed constant behavior of the diffractive elements and of the interferometer with temporal frequency (or wavelength). Both assumptions are, of course, not true in general. The topological phase of a diffractive element is wavelength dependent, and so is the self-imaging distance for the interferometric setup. Hence for broadband signals consisting of femtosecond pulses an exact description would have to take these effects into account. For practical implementations, one might possibly also have to consider additional effects such as material dispersion. Quasi-monochromatic behavior may be assumed as long as the bandwidth of the signal  $\Delta v$  is much smaller than the center frequency  $\bar{v}_t$ .  $\Delta v$  is, in turn, given as the inverse of the signal pulse duration,  $\tau_p$ . We may distinguish two cases: first,  $\tau_p > \tau_1$  and second,  $\tau_p < \tau_1$ . The first case, in which the typical time delay of

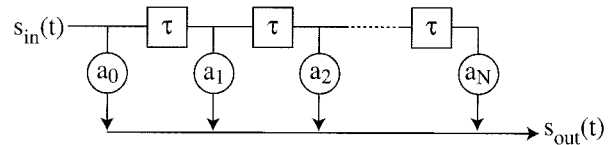


Fig. 3. Schematic of a tapped-delay-line filter. Here constant delays of duration  $\tau$  are shown. The weights in the branches are denoted  $a_m$ .

the filter is shorter than the pulse duration, is typical for signal-processing applications (see Section 5 below). In the second case, however, the interferometer would generate a sequence of individual output pulses from a single input pulse. Obviously, the assumption of quasi-monochromaticity is more easily satisfied in the first case.

## 5. Modeling of a Double-Diffraction Experiment as a Tapped-Delay-Line Filter

In the language of linear systems theory, Eq. (49) represents a tapped-delay-line (or finite-impulse-response) filter that can be used to implement discrete convolutions. A finite-impulse-response filter is shown schematically in Fig. 3. Incoming signal  $s(t)$  is split into  $N$  branches. The branches are weighted and are then recombined. We point out specific properties of a double-diffraction setup: Notably, the weighting factors are nonnegative if the two elements are implemented as phase-complementary elements and the output is observed in the zeroth order. Also, in Ref. 5 it was pointed out that one may also place the detector in another output order, in which case the weighting factors are mathematically expressed as discrete convolutions. Then they may assume negative or even complex values; however, their design may become awkward.

## 6. Implementations of Double-Diffraction Systems and Outlook for the Future

Several implementations of double-diffraction setups exist. Well-known examples are the Gires–Tournois interferometer<sup>10,11</sup> and the  $4f$  system for pulse shaping.<sup>12–14</sup> Figures 4–6 show several generic optical setups. Figure 4 is based on conventional  $4f$  imaging (called version 1). Figure 4a shows a transmissive version consisting of two refractive lenses. For systems that work with picosecond and femtosecond pulses a diffraction-based filter might be used to

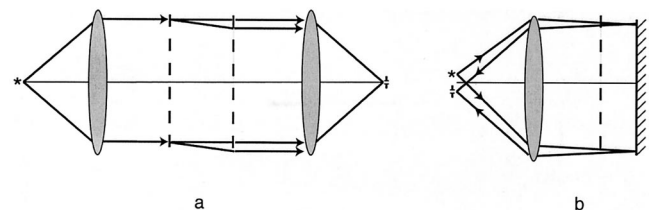


Fig. 4. Version 1 of a double-diffraction setup based on a  $4f$  imaging system: a, transmissive system with two refractive lenses; b, refractive–reflective version obtained by placing a mirror in the Fourier plane.

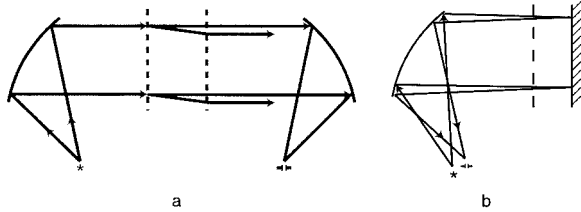


Fig. 5. Version 2 of a double-diffraction setup: purely reflective  $4f$  systems with a, two parabolic mirrors and b, one parabolic mirror and a planar mirror in the Fourier plane.

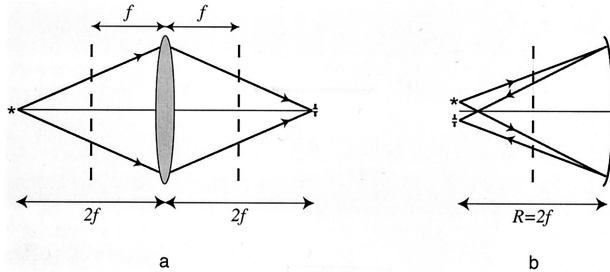


Fig. 6. Version 3 of a double-diffraction setup based on  $2f$ - $2f$  imaging systems: a, a system that uses a refractive lens in transmission and b, a purely reflective system.

reduce or to completely eliminate material dispersion. One does this for version 1 by placing a flat mirror in the Fourier plane [Fig. 4b]. Figures 5 and 6 show different variations of this scheme. Figure 5 (version 2) is a purely reflective system: a shows the analog of version 1a and consists of two parabolic mirrors and b is the reflective analog of version 1b. Finally, in Fig. 6 the telecentric  $4f$  setup is replaced by a single lens imaging system (version 3). In this case, self-imaging with a noncollimated beam is used. Figures 6a and 6b represent the analogs of versions 1a and 1b, respectively.

Applications of double-diffraction devices may exist in temporal filtering of ultrafast signals. For short distances between the two masks, i.e., small values of  $M$ , the time delays are in the femtosecond range; thus the applications of a double-diffraction device will be limited to optical frequencies. For applications in the terahertz domain, time delays of the order of a picosecond are required. Devices with such a large separation between  $M_1$  and  $M_2$  may be implemented in a waveguide-optical configuration, as suggested earlier by Bryngdahl<sup>15</sup> and Ulrich.<sup>16</sup>

For spectral applications, interesting implementa-

tions may be found along the lines of Ref. 17, in which the “emulation” of a Lyot–Öhman filter by means of a cascade of Talbot cells of suitable lengths was suggested. Our interest in this approach to double diffraction is to a large extent based on the possibility of using lithographically generated diffraction masks. Such masks would allow one to implement a variety of impulse responses and thus would offer the possibility of flexibility in filter design.

## References

1. H. F. Talbot, “Facts relating to optical science,” *Phil. Mag.* **9**, 401–407 (1836).
2. E. Lau, “Beugungserscheinungen an Doppelrastern,” *Ann. Phys. (Leipzig)* **2**, 417–423 (1948).
3. A. W. Lohmann and D. E. Silva, “An interferometer based on the Talbot effect,” *Opt. Commun.* **2**, 413–415 (1971).
4. J. Jahns and A. W. Lohmann, “The Lau effect (a diffraction experiment with incoherent illumination),” *Opt. Commun.* **28**, 263–267 (1979).
5. J. Jahns, E. El Joudi, D. Hagedorn, and S. Kinne, “Talbot interferometer as a time filter,” *Optik (Stuttgart)* **112**, 295–298 (2001).
6. J. Jahns, H. Knuppertz, and A. W. Lohmann, “Montgomery self-imaging effect using computer-generated diffractive optical elements,” *Opt. Commun.* **225**, 13–17 (2003).
7. W. D. Montgomery, “Self-imaging objects of infinite aperture,” *J. Opt. Soc. Am.* **57**, 772–778 (1967).
8. A. W. Lohmann and D. Mendlovic, “Temporal filtering with time lenses,” *Appl. Opt.* **31**, 6212–6219 (1992).
9. B. E. A. Saleh and M. C. Teich, *Fundamentals of Photonics* (Wiley, New York, 1991).
10. F. Gires and P. Tournois, “Interféromètre utilisable pour la compression d’impulsions lumineuses modulées en fréquences,” *C. R. Acad. Sci.* **258**, 6112–6115 (1964).
11. E. B. Treacy, “Optical pulse compression with diffraction gratings,” *IEEE J. Quantum Electron.* **QE-5**, 454–458 (1969).
12. C. Froehly, B. Colombeau, and M. Vampouille, “Shaping and analysis of picosecond light pulses,” in *Progress in Optics*, E. Wolf, ed. (North-Holland, Amsterdam, 1983), Vol. 20, pp. 63–153.
13. A. M. Weiner, J. P. Heritage, and E. M. Kirschner, “Encoding and decoding of femtosecond pulses,” *Opt. Lett.* **13**, 300–302 (1988).
14. P.-C. Sun, K. Oba, Y. T. Mazurenko, and Y. Fainman, “Space-time processing with photorefractive volume holography,” *Proc. IEEE* **87**, 2086–2097 (1999).
15. O. Bryngdahl, “Image formation using self-imaging techniques,” *J. Opt. Soc. Am.* **63**, 416–419 (1973).
16. R. Ulrich and G. Ankele, “Self-imaging in homogeneous planar optical waveguides,” *Appl. Phys. Lett.* **27**, 337–339 (1975).
17. A. W. Lohmann, J. Ojeda-Castañeda, and E. E. Sicre, “Multiple interaction bandstop filters based on the Talbot effect,” *Opt. Commun.* **49**, 388–392 (1984).